Long noncoding RNA H19 regulates degeneration and regeneration of injured peripheral nerves

Yu-Mei Feng[1, #], Jian Shao[1, #], Min Cai[2], Yi-Yue Zhou[1], Yi Yao[3], Jia-Xi Qian[1], Zi-Han Ding[1], Mao-Rong Jiang[1], Deng-Bing Yao[1, *]

https://doi.org/10.4103/1673-5374.363182

Date of submission: May 23, 2022

Date of decision: September 9, 2022

Date of acceptance: November 20, 2022

Date of web publication: December 21, 2022

From the Contents

Graphical Abstract

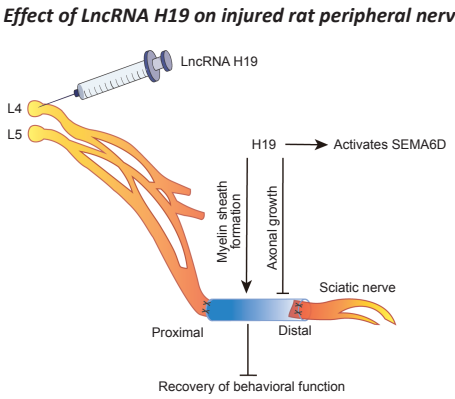

Abstract

Our previous studies have shown that long noncoding RNA (lncRNA) H19 is upregulated in injured rat sciatic nerve during the process of Wallerian degeneration, and that it promotes the migration of Schwann cells and slows down the growth of dorsal root ganglion axons. However, the mechanism by which lncRNA H19 regulates neural repair and regeneration after peripheral nerve injury remains unclear. In this study, we established a Sprague-Dawley rat model of sciatic nerve transection injury. We performed *in situ* hybridization and found that at 4–7 days after sciatic nerve injury, lncRNA H19 was highly expressed. At 14 days before injury, adeno-associated virus was intrathecally injected into the L4–L5 foramina to disrupt or overexpress lncRNA H19. After overexpression of lncRNA H19, the growth of newly formed axons from the sciatic nerve was inhibited, whereas myelination was enhanced. Then, we performed gait analysis and thermal pain analysis to evaluate rat behavior. We found that lncRNA H19 overexpression delayed the recovery of rat behavior function, whereas interfering with lncRNA H19 expression improved functional recovery. Finally, we examined the expression of lncRNA H19 downstream target SEMA6D, and found that after lncRNA H19 overexpression, the SEMA6D protein level was increased. These findings suggest that lncRNA H19 regulates peripheral nerve degeneration and regeneration through activating SEMA6D in injured nerves. This provides a new clue to understand the role of lncRNA H19 in peripheral nerve degeneration and regeneration.

Key Words: adeno-associated virus; dorsal root ganglion; lncRNA H19; nerve degeneration; nerve regeneration; peripheral nerve; rat; sciatic nerve injury; semaphorin 6D; Wallerian degeneration

Introduction

Peripheral nerves throughout the body are vulnerable to various injuries, such as traction injury, crush injury, and impact injury (Robinson, 2000). Peripheral nerve injury causes a high disability rate, which places a heavy burden on society and families. Repairing peripheral nerve injury is a large clinical challenge. Despite many efforts, repair outcomes after injury are not satisfactory (Siemionow and Brzezicki, 2009). Strategies to promote nerve regeneration remain a major issue for the field.

Axons of damaged neurons in the peripheral nervous system have the ability to regenerate after injury. When axons in the peripheral nervous system are damaged, axonal degeneration, myelin degeneration and disintegration occur rapidly in the distal stump, a process called Wallerian degeneration (WD) (Li et al., 2021). Studies have shown that WD is the natural immune response of peripheral nerves to injury, and that rapid removal of degenerated axons and myelin sheath debris is conducive to promoting axon regeneration (Geuna et al., 2009; Dubový, 2011; Lu et al., 2022). During nerve regeneration, Schwann cells (Nocera and Jacob, 2020) and infiltrated and polarized macrophages (Chen et al., 2015) accumulate in large numbers at the injured site to phagocytose and remove the degenerated axon and myelin sheath debris; the digestion is largely completed by the second week after injury. In this favorable microenvironment, the axon regeneration rate can reach approximately 1 mm per day, but this rate of regeneration is low, and functional recovery is not good (Chan et al., 2014). Nerve regeneration and the reinnervation of target organs depend on the ability of neurons with damaged axons to survive and regenerate (Navarro et al., 2007). Sciatic nerve injury (SNI) is a representative model for studying peripheral nerve injury. Sciatic nerve axons are derived from the L4 and L5 dorsal root ganglion (DRG). In the model, these axons are squeezed or transected, which leads to neuronal damage or death (Tang and Brimijoin, 2002), and the internal regeneration process of surviving neurons is activated, which promotes axonal regeneration and the reconstruction of nerve fiber structure and function (Duan et al., 2018; Tang, 2020). This process involves changes in a variety of related factors and signaling pathways in neurons. Myelin-related genes in Schwann cells and DRGs are downregulated, while growth-related genes are upregulated. However, the gene expression is weak and over time cannot support axon regeneration. Therefore, the axon may not be able to successfully connect the original target organ (Gordon, 2020). Therefore, we aim to investigate how to promote axon regeneration and help it to quickly find the correct target organ within a limited time. Studying these changes is very important in the promotion of nerve regeneration.

[1]School of Life Sciences, Key Laboratory of Neuroregeneration of Jiangsu and Ministry of Education, Coinnovation Center of Neuroregeneration, Nantong University, Nantong, Jiangsu Province, China; [2]Medical School of Nantong University, Nantong, Jiangsu Province, China; [3]Nantong University Xinglin College, Nantong, Jiangsu Province, China

*Correspondence to: Deng-Bing Yao, MD, PhD, yaodb@ntu.edu.cn.

https://orcid.org/0000-0002-5177-0318 (Deng-Bing Yao)

#Both authors contributed equally to this work.

Funding: *The study was supported by the National Natural Science Foundation of China, Nos. 31971277 (to DBY), 31950410551 (to DBY); Scientific Research Foundation for Returned Scholars, Ministry of Education of China (to DBY); a project funded by the Priority Academic Program Development of Jiangsu Higher Education Institutions (PAPD) (to DBY); the Postgraduate Research & Practice Innovation Program of Jiangsu Province of China, No. KYCX 19-2050 (to JS); and Jiangsu College Students' Innovation and Entrepreneurship Training Program, No. 202213993005Y (to YY).*

How to cite this article: *Feng YM, Shao J, Cai M, Zhou YY, Yao Y, Qian JX, Ding ZH, Jiang MR, Yao DB (2023) Long noncoding RNA H19 regulates degeneration and regeneration of injured peripheral nerves. Neural Regen Res 18(8):1847-1851.*

Long noncoding RNAs (lncRNAs) are a class of noncoding RNAs that lack a remarkable open reading frame and were initially considered transcription noise (Gibb et al., 2011). On the basis of their genomic position relative to adjacent protein-coding genes, lncRNAs can be divided into the following five categories: sense, antisense, bidirectional, intron and intergenic lncRNAs (Peng et al., 2018). In general, lncRNAs do not encode proteins or encode only a few proteins, most of which participate in gene regulation in the form of RNA (Rinn and Chang, 2012). Increasing evidence indicates that lncRNAs may affect the processes of cell development and disease (Esteller, 2011; Fatica and Bozzoni, 2014). In the nervous system, lncRNAs are involved in brain development, neuronal maintenance and differentiation, synaptic plasticity, and the recovery of cognitive and memory function (Wu et al., 2013; Shi et al., 2019). Abnormal lncRNAs have also been found in many neurodegenerative diseases, such as Alzheimer's disease and Parkinson's disease (Wan et al., 2017).

In a previous study, our research group found that the expression of lncRNA H19 (H19) was upregulated during WD through bioinformatics and gene chip analyses, suggesting that H19 may play a regulatory role during nerve regeneration (Li et al., 2022). H19 was the first lncRNA gene discovered, and H19 has paternal imprints and mainly expresses maternal genes. In humans, H19 transcribes a 2.3 kb noncoding RNA transcript LncRNA H19 is highly expressed during embryonic development, and its expression decreases in most tissues after birth (Feil et al., 1994). Previous studies have shown that H19 is a predictor of poor prognosis for many diseases (Peng et al., 2017; Zhao et al., 2017; Huang et al., 2018). H19 downregulation remarkably inhibits tumor growth (Zhou and Zhang, 2020). H19 is also abnormally expressed in many cancers, such as breast cancer (Adriaenssens et al., 1998), gastric cancer (Chen et al., 2016), colon cancer (Li et al., 2016), hepatocellular carcinoma (Niu et al., 2017), kidney cancer (Wang et al., 2015), lung cancer (Matouk et al., 2015), and cervical cancer (Feigenberg et al., 2013). However, there are few studies on H19 in the field of nerve injury and regeneration. Li et al. (2022) reported that H19 promoted Schwann cell migration and slowed DRG axon growth *in vitro*, and predicted the target genes of H19. In this study, target gene semaphorin 6D (SEMA6D) was selected for follow-up studies. We constructed an intrathecal injection model in Sprague Dawley rats, and injected adeno-associated virus (AAV) *in vivo* to overexpress or interfere with H19. The purpose of this study was to investigate how H19 affects SNI and nerve regeneration *in vivo*, which is of great significance for the subsequent study of the molecular mechanism of H19 in nerve regeneration.

Methods

Animal models

All protocols used in this study were approved by the Institutional Animal Care and Use Committee of Nantong University, China (approval No. 20190301-004) on May 9, 2019. All animal tests were conducted according to the Guide for the Care and Use of Laboratory Animals (8th ed; National Research Council of the National Academies, 2011). All experiments were designed and reported according to the Animal Research: Reporting of *In Vivo* Experiments (ARRIVE) guidelines (Percie du Sert et al., 2020).

The experimental animals used in this study were obtained from the Experimental Animal Center of Nantong University (license No. SCXK (Su) 2019-0001). Hormones in female rats may affect nerve repair (17β-estradiol has been reported to promote remyelination in injured sciatic nerves (Gu et al., 2018)), and male rats have a more docile personality, which is conducive to smooth experiments. Thus, in this study, we used specific pathogen-free Sprague Dawley male rats, weighing 180–200 g, aged 2–8 weeks. Initially, we detected H19 expression at 0 (immediately), 1, 4, 7, 14, 21, and 28 days after SNI (n = 3/time point). Then, AAV-pH19 transfection efficiency in DRG tissues was determined immediately, at 12 hours, and 1, 4, 7, 14, 21, 28, 35, 42, 49, and 56 days after SNI (n = 3/time point). Finally, an additional 48 rats were randomly divided into the following four groups: interference control group (NC-sh), interference group (AAV-shH19), overexpression control group (NC-p) and overexpression group (AAV-pH19) (n = 12/group) to determine whether H19 affects SNI and nerve regeneration *in vivo*.

NC-sh and NC-p (both from Obio Technology Shanghai Corp., Ltd., Shanghai, China) were the controls of interference and overexpression of H19, respectively, and they were constructed using different vectors. Others were used to detect the expression of H19. At 14 days before modeling, the rats were weighed and injected intraperitoneally with compound anesthetics (51.95 mL ddH_2O, 33.8 mL propylene glycol [Xilong Scientific, Guangdong, China], 14.25 mL anhydrous ethanol [Shanghai Lingfeng Chemical Reagent Co., Ltd. Shanghai, China], 4.25 g chloral hydrate [Shanghai Lingfeng Chemical Reagent Co., Ltd.], 2.12 g magnesium sulfate [Shanghai Lingfeng Chemical Reagent Co., Ltd.], 0.886 g sodium pentobarbital [Sigma-Aldrich, St. Louis, MO, USA]) at 0.3 mL/100 g body weight. After complete anesthesia was induced, the dorsal skin of each rat was shaved, and the skin was cut open after disinfection with iodovol. Intrathecal injection was performed in the L4 to L5 intervertebral space. A total of 15–20 μL modified AAV (titer of approximately 1×10^{12}, Obio Technology Shanghai Corp., Ltd.) was injected with a microliter syringe (Gaoge, Shanghai, China). When the virus was injected into the spinal cord, the rat flicked its tail. After the wound was sutured using 4-0 sutures, the rat was placed in a laboratory with an environmental barrier (20°C, 40% humidity, 12-hour light/dark cycle, five rats in each cage).

The sciatic nerve transection model was established as follows. After complete anesthesia was induced, the left leg of the rat was shaved. After iodophor disinfection, the skin was cut at 45° from the leg bone with surgical scissors, and the muscles were separated to expose the sciatic nerve. The sciatic nerve was transected, and a 0.5-cm silicone tube (Invitrogen, New York, NJ, USA) was sutured between the two stump ends to assist the growth of the new axon (**Additional Figure 1**). The rats were sutured and placed in a laboratory with an environmental barrier. The main experimental flow chart is shown in **Additional Figure 2**.

Tissue harvesting

Sciatic nerve

The sciatic nerve was transected as follows. After complete anesthesia was induced, the sternum was cut to expose the heart, the pointed part of the needle was removed, and the needle was inserted into the left ventricle of the rat until the aorta was penetrated. Then, 0.9% normal saline was injected and the right atrial appendage was cut to speed up the bleeding. After the liver and other parts changed from red to white, 4% formaldehyde was used and perfusion was stopped after the body became stiff. The sciatic nerve was separated from the silicone tube and placed in a centrifuge tube containing 4% formaldehyde solution at 4°C overnight. Then, it was dehydrated in a gradient of 10%, 20% and 30% sucrose solution. The dehydrated sciatic nerve was cut neatly with a blade and then placed on a sample tray, and optimal cutting temperature compound was added to rapidly freeze the tissue. The tissue was cut into 12-μm-thick sections using a Leica CM3050 S cryostat (Leica-Microsystems, Shanghai, China). The slices were adhered to slides, placed in a drying box at 37°C for 8–10 hours, and then frozen in a –80°C freezer.

L4 and L5 DRG

After rats were injected with a compound anesthetic, the iliac bone of rat were broken with hemostatic forceps. After the sciatic nerve was located, the L4 and L5 DRG tissues were slowly removed with hemostatic forceps, the excess nerves were cut off, and the DRG tissue was placed into labeled cryotubes and stored at –80°C.

Fluorescence *in situ* hybridization

The sciatic nerve slices were baked at 50°C for 55 minutes and fixed in 4% paraformaldehyde. The slices were washed twice with phosphate buffered saline, treated with protease K, and then fixed with 4% paraformaldehyde. Then, the slices were prehybridized at 42°C for 3 hours and hybridized for 12 hours. The cells were washed with 4×, 2×, and 1× saline sodium citrate (SSC) mixed solution supplemented with 0.1% Tween 20. 4′,6-Diamidino-2-phenylindole (DAPI, Abcam, ab104139) mounting solution was added dropwise and stained for 30 minutes. Images were taken using a Zeiss Axioscope 5 fluorescence imaging microscope (Carl Zeiss AG, Guangzhou, China).

Immunofluorescence staining

The intact sciatic nerve sections at 28 days were selected and washed twice for 10 minutes each with phosphate buffered saline containing Tween 20. Blocking solution (Coolaber, Beijing, China, SL1336) was added dropwise to the circled area by PAP Pen (Daito Sangyo Co. Ltd., Daito city, Osaka, Japan) and incubated at 24°C for 2 hours. The nerve sections were incubated with primary antibody β-tubulin III (axon marker, mouse, 1:1000, Abcam, Cambridge, UK, Cat# ab78078, RRID: AB_2256751) at 4°C for 12 hours, incubated with goat anti-mouse IgG Cy3 (1:400, Proteintech Group, Chicago, IL, USA, Cat# SA00009-1, RRID: AB_2814746) at room temperature for 2 hours in the dark, and then washed with phosphate buffered saline three times for 10 minutes each. DAPI sealing solution was dropped onto the slide, and the slide was covered slowly to avoid bubbles. The slides were placed in a dark box and temporarily stored at 4°C for approximately 1 week to protect against fluorescence quenching. The fluorescence intensity of β-tubulin III was observed under a Zeiss Axioscope 5 fluorescence imaging microscope.

Real-time polymerase chain reaction

TRI Reagent (Ambion) was used to extract total RNA from L4 and L5 DRG tissue at 0, 0.5, 1, 4, 7, 14, 21, 28, 35, 42, 49 and 56 days after infection with AAV, and an RT Kit (Dongsheng Biotech) was used to prepare complementary DNA (cDNA) from the total RNA. Then, a real-time PCR system (Applied Biosystems, Foster City, CA, USA) was used for analysis. We repeated these experiments three times using different batches of Sprague Dawley rats, and glyceraldehyde-3-phosphate dehydrogenase (GAPDH) was used as an internal control for standardization. The comparative cycle threshold method (Li et al., 2018) was used to evaluate the relative expression. PCR amplification was performed according to the following parameters: stage 1: 95°C for 2 minutes; stage 2: 94°C for 15 seconds, 60°C for 60 seconds, 35 cycles; stage 3: 95°C for 15 seconds, 60°C for 60 seconds, 95°C for 15 seconds. The sequences of the PCR primers used are shown in **Table 1**.

Table 1 | **Main primers used for the real-time polymerase chain reaction assay**

Gene	Sequence
H19	Forward: 5'-TGT CAA CAG GAA GGG AAC GG-3'
	Reversed: 5'-CAG CTG CTT TAC CTC GCT CT-3'
GAPDH	Forward: 5'-GCA AGT TCA ACG GCA CAG-3'
	Reversed: 5'-CGC CAG TAG ACT CCA CGA C-3'

GAPDH: Glyceraldehyde-3-phosphate dehydrogenase; H19: long noncoding RNA H19.

Western blot analysis
The DRG tissues infected with AAV for 7 and 14 days were dissolved in lysis buffer containing protease inhibitors. The supernatant containing protein was collected after centrifugation. The proteins were separated by 10% sodium dodecyl sulfate polyacrylamide gel electrophoresis and transferred to polyvinylidene fluoride membranes. The membrane was blocked in 5% skim milk for 2 hours and then incubated overnight at 4°C with primary antibodies against SEMA6D (mouse, 1:2000, Santa Cruz Biotechnology, Hercules, CA, USA, Cat# sc-393258) and GAPDH (rabbit, 1:1000, Sigma-Aldrich, Cat# G8795, RRID: AB_1078991). Then, the membrane was incubated with secondary antibodies goat anti-mouse IgG (1:1000, BioRad, Hercules, CA, USA, Cat# 103001, RRID: AB_609693) and horseradish peroxidase-labeled goat anti-rabbit IgG (1:1000, Beyotime, Shanghai, China, Cat# A0208, RRID: AB_2892644) at 24°C for 2 hours. The relative protein levels were expressed as an optical density ratio to GAPDH, and the experiment was repeated three times using different batches of rats.

Behavioral experiments
Before the behavioral experiments, the rats had adaptive training for 1 week.

Gait analysis
A CatWalk gait analyzer (Noldus Information Technology b.v., Leesburg, VA, USA) was used to capture gait data, such as footprints, recorded by a CatWalk fluorescent plate at 2, 4 and 8 weeks following sciatic nerve transection after virus injection. CatWalk XT 10.6 was used to analyze the postoperative recovery of rats. The paw length (PL), toe spread (TS), and intermediary toe spread (IT) of the normal (N) and the experimental (E) hind legs were measured by footprints. The sciatic function index (SFI) was calculated using the following formula (Tang et al., 2013): SFI = 109.5 (ETS – NTS) / NTS – 38.3 (EPL – NPL) / NPL + 13.3 (EIT – NIT) / NIT – 8.8. SFI = –100 indicates that the toe had not recovered. The closer SFI is to 0, the better the recovery of the toe.

Thermal pain analysis
The thermal pain response of rats was used to investigate the repair of thermosensation at 2, 4 and 8 weeks after SNI and virus injection. The rats were irradiated with a constant light source (IITC Life Sciences, Woodland Hills, CA, USA), and the time for contraction after light stimulation was recorded. The upper limit was 30 seconds to avoid tissue damage.

Transmission electron microscope analysis
At 2, 4 and 8 weeks after SNI, the sciatic nerve wrapped in the silicone tube was removed, fixed in glutaraldehyde, post-fixed with osmium tetroxide (Sigma), dehydrated by ethanol gradient, embedded with epoxy resin, and then sectioned. After staining, the regeneration and repair of the myelin sheath at the distal end of the sciatic nerve were observed by transmission electron microscopy (CM-120; Philips, Amsterdam, The Netherlands), and the number of myelin layers was calculated.

Statistical analysis
GraphPad Prism (version 6.02, GraphPad Software, San Diego, CA, USA, www.graphpad.com) was used for statistical analysis. Differences between two groups were compared using Student's *t*-test. All data are expressed as the mean ± standard deviation. $P < 0.05$ was considered statistically significant.

Results

Expression of lncRNA H19 in injured sciatic nerves
H19 expression during the WD process after SNI was detected at seven time points by fluorescence *in situ* hybridization. H19 expression level was higher at 4–7 days than that at 0 days after SNI and decreased gradually after 14 days (**Figure 1**).

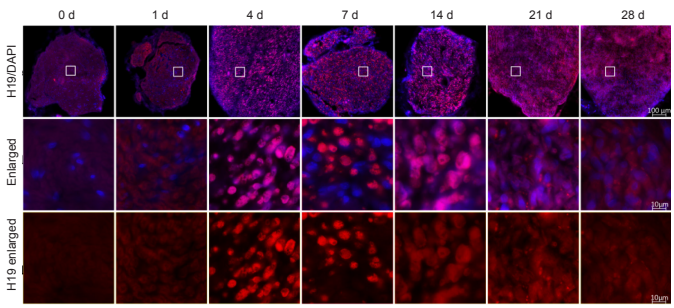

Figure 1 | Fluorescence *in situ* hybridization results of lncRNA H19 on the distal stump of the rat sciatic nerve.
LncRNA H19 expression (red) in the sciatic nerve. The fluorescence intensity was highest at 4 and 7 days. Nuclei were labeled by DAPI (blue). Scale bars: 100 μm (upper rows) and 10 μm (lower two rows). DAPI: 4′,6-Diamidino-2-phenylindole; lncRNA H19: long noncoding RNA H19.

AAV efficiency of lncRNA H19 is verified *in vivo*
The AAV transfection efficiency of H19 in DRG tissue after SNI was analyzed by real-time polymerase chain reaction (**Figure 2**). The AAV interference or overexpression efficiency of H19 was significantly higher in DRG tissue than in the control group ($P < 0.05$).

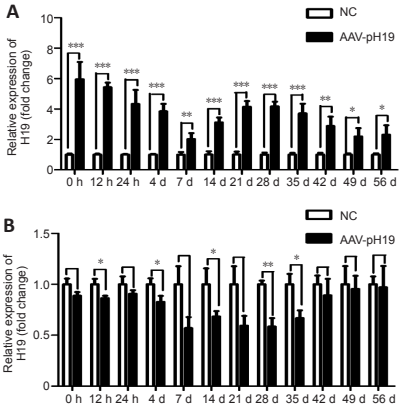

Figure 2 | *In vivo* verification of AAV transfection efficiency of lncRNA H19.
(A) AAV-pH19 transfection efficiency in dorsal root ganglion (DRG) at different time points. (B) AAV-shH19 transfection efficiency in DRG tissues at different time points. Data normalized by NC group are expressed as mean ± SD ($n = 3$). *$P < 0.05$, **$P < 0.01$, ***$P < 0.001$ (Student's *t*-test). AAV: Adeno-associated virus; lncRNA H19: long noncoding RNA H19.

Overexpression of lncRNA H19 affects axon growth of the sciatic nerve after injury
On the 14th day after injury, axon growth of the distal sciatic nerve stump was detected using immunohistochemistry (**Figure 3**). When H19 was overexpressed, axon growth was worse and the fluorescence intensity of SCG10 labeled new axons was weaker than that in the control group ($P < 0.05$). The results suggested that H19 overexpression inhibited axon regeneration.

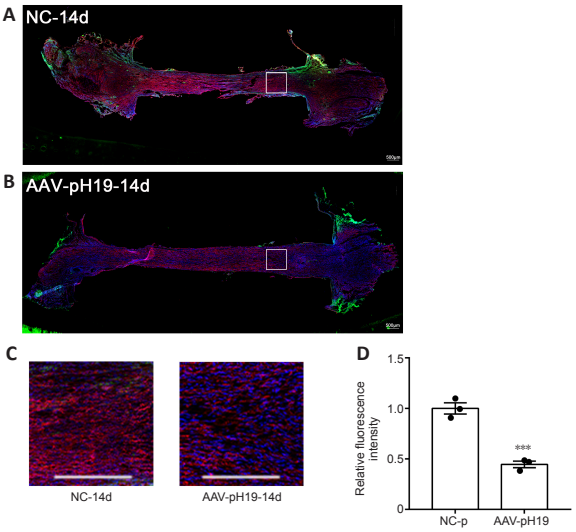

Figure 3 | Overexpression of H19 affects sciatic nerve axon regeneration at 14 days after sciatic nerve transection.
(A, B) The growth of axons in the NC-p (A) and AAV-pH19 groups. (C) Local magnified view of the distal sciatic nerve. Immunofluorescence staining of β-tubulin III (red, stained by Cy3) and AAV (green) for H19 overexpression. Fluorescence intensity of the overexpression group was weaker than that of control group. Nuclei were stained with DAPI (blue). Scale bars: 500 μm. (D) Quantification of relative fluorescence intensity (normalized by NC-p group). Data are expressed as mean ± SD ($n = 3$). ***$P < 0.001$, *vs.* NC-p group (Student's *t*-test). AAV: Adeno-associated virus; DAPI: 4′,6-diamidino-2-phenylindole; H19: long noncoding RNA H19.

LncRNA H19 interference or overexpression affects the regeneration and repair of the nerve myelin sheath
The newborn sciatic nerve tissue in the distal sciatic nerve myelin was observed by transmission electron microscopy at 2, 4, and 8 weeks after SNI. The peripheral nerve myelin sheath showed a light and dark concentric circular plate-like structure. At 2, 4, and 8 weeks, after interference with H19, the number of myelin sheaths was lower, the myelin sheath was thinner, and the number of myelin layers was reduced compared with those in the control group. Overexpression of H19 had the opposite effects (**Figure 4**).

LncRNA H19 interference or overexpression affects the behavior of rats
Motor function
The CatWalk gait technique was used to detect motor function recovery in rats. After interference with H19, the SFI value was higher than that in the NC-sh group at 2 and 4 weeks. At 8 weeks, the difference between the two groups was not significant. After overexpression of H19, the SFI value was lower than that in the NC-p group at 2 and 4 weeks. At 8 weeks, the difference between the two groups was not significant (**Figure 5**).

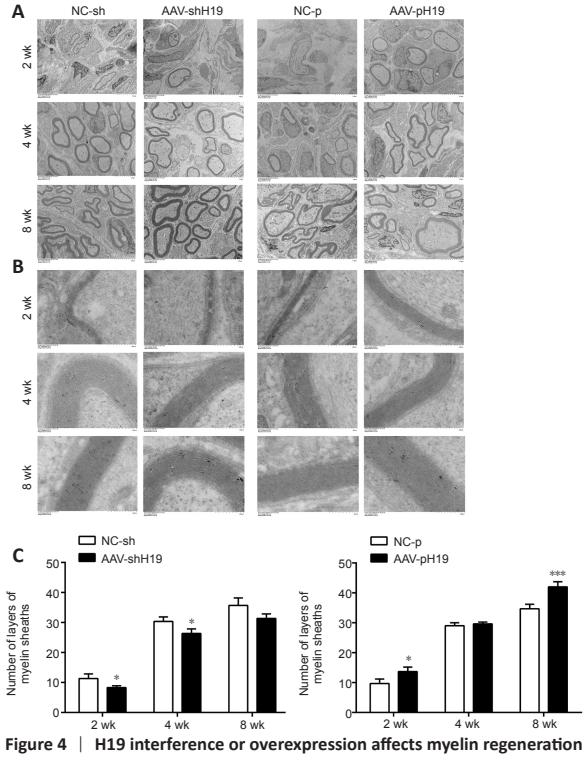

Figure 4 | H19 interference or overexpression affects myelin regeneration after sciatic nerve transection.

(A) Electron microscopy of the number of myelin sheaths after sciatic nerve transection and H19 interference or overexpression. (B) Enlarged image of A. Compared with that of the control group, myelin sheath number was decreased after H19 intervention. Scale bars: 10 μm (A), 500 nm (B). (C) Quantification of the number of broad layers in B. Data are expressed as mean ± SD (n = 3). *P < 0.05, ***P < 0.001, *vs.* NC-sh or NC-p group (Student's t-test). AAV: Adeno-associated virus; H19: long noncoding RNA H19.

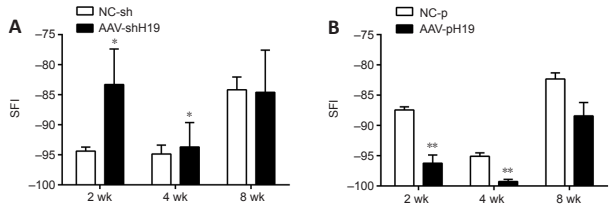

Figure 5 | H19 interference or overexpression affects the motor function of rats with sciatic nerve transection.

A greater SFI indicates better recovery of motor function. (A) SFI of rats at 2, 4, and 8 weeks after sciatic nerve transection and H19 interference. (B) SFI of rats at 2, 4 and 8 weeks after sciatic nerve transection after H19 overexpression. Data are expressed as mean ± SD (n = 3). *P < 0.05, **P < 0.01, *vs.* NC-sh or NC-p group (Student's t-test). AAV: Adeno-associated virus; H19: long noncoding RNA H19.

Thermal pain response

We investigated thermosensation after SNI in rats. After interference with H19, the contraction reaction time of rats at 2 and 4 weeks was shorter than that in the negative control group, whereas the contraction reaction time at 8 weeks was similar. After overexpression of H19, the contraction time of rats at 2 and 4 weeks was longer than that in the control group, whereas the contraction reaction time was similar at 8 weeks (**Figure 6**).

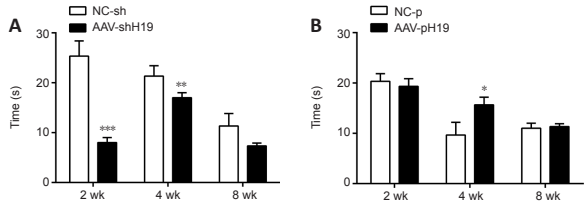

Figure 6 | Effects of H19 interference or overexpression on the thermal pain response of rats.

(A) Thermal pain response time of rats at 2, 4, and 8 weeks after sciatic nerve transection and H19 interference. (B) Thermal pain response time of rats at 2, 4, and 8 weeks after sciatic nerve transection and H19 overexpression. Data are expressed as mean ± SD (n = 3). *P < 0.05, **P < 0.01, ***P < 0.001, *vs.* NC-sh or NC-p group (Student's t-test). AAV: Adeno-associated virus; H19: long noncoding RNA H19.

Protein expression of lncRNA H19 target gene *SEMA6D*

In a previous study, through Gene Ontology function analysis, we predicted the target genes related to H19 during the process of nerve regeneration (Li et al., 2022). SEMA6D, an axon guiding factor, was among the predicted H19 target genes, and we speculate that there is a certain correlation between H19 and SEMA6D. Proteins in DRG tissue were extracted at 7 and 14 days after H19 interference or overexpression and SNI. Western blotting was used to investigate the changes in SEMA6D protein expression during nerve regeneration. After H19 interference, SEMA6D protein expression was lower than that in the NC-sh group at 7 and 14 days, and after H19 overexpression, SEMA6D protein expression was higher than that in the NC-p group (**Figure 7**). Because our results indicate that H19 inhibits axon growth, we speculate that H19 may activate SEMA6D, thereby affecting axon growth.

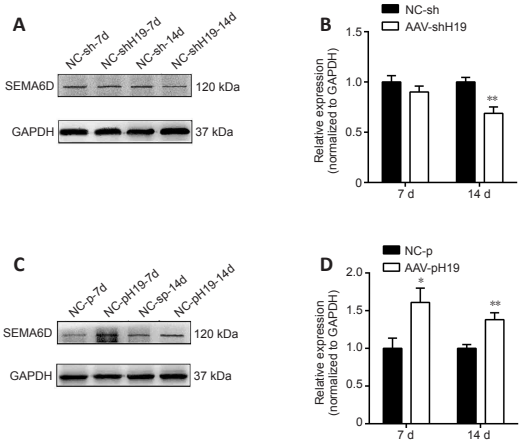

Figure 7 | Protein expression changes of SEMA6D after H19 interference or overexpression.

(A) Protein expression changes of SEMA6D after H19 interference at 7 and 14 days. (B) Quantification of SEMA6D expression after H19 interference at 7 and 14 days, standardized by GAPDH. (C) Protein expression changes in SEMA6D after H19 overexpression at 7 and 14 days. (D) Quantification of SEMA6D expression after H19 overexpression at 7 and 14 days, standardized by GAPDH. Data are expressed as mean ± SD (n = 3). *P < 0.05, **P < 0.01, *vs.* NC-sh or NC-p group (Student's t-test). AAV: Adeno-associated virus; GAPDH: glyceraldehyde-3-phosphate dehydrogenase; H19: long noncoding RNA H19; SEMA 6D: semaphorin 6D.

Discussion

This study investigated the role of H19 in nerve regeneration. Using a sciatic nerve transection model, we found that H19 expression was higher in rats 4–7 days after SNI. The changes in H19 expression suggest that H19 may be a factor in neural regeneration. Subsequently, we constructed AAV vectors to either interfere with or overexpress H19. After constructing an intrathecal injection model *in vivo* and transecting the sciatic nerve, we found through tissue immunofluorescence staining that the growth of new axons in the sciatic nerve after H19 overexpression was weaker than that in the control group. Thus, H19 may inhibit axon growth in the sciatic nerve. The number of myelin sheaths in the sciatic nerve was increased after H19 overexpression, and H19 interference had the opposite effect, suggesting that H19 promotes myelin sheath formation in the sciatic nerve. At the same time, H19 can regulate myelination protection by retaining part of myelin (Spinelli et al., 2021), suggesting that it may be related to the mechanism by which H19 promotes myelination. New axons grow many branches, but not all branches find the corresponding target organs, and those branches tend to undergo collapse (Dharap et al., 2009). We hypothesize that H19 inhibits the growth of these misdirected axon branches. Furthermore, H19 promoting myelination suggests that H19 may promote the growth of correctly oriented axonal myelin sheaths.

The CatWalk gait analysis system captures rat footprints and objectively detects gait behavior. SFI analysis indicated that rat motor function recovery after H19 overexpression was poor. Using a constant light source to irradiate the injured hind limbs of rats, we found that the contraction time of rats with H19 overexpression was longer than that of the control group, whereas motor function recovery with H19 interference was better and the contraction reaction time was shorter. These results suggest that H19 affects the recovery of behavioral function after SNI in rats.

In a previous study, gene chip analysis and lncRNA H19 Gene Ontology function prediction analysis showed that SEMA6D is a downstream target gene of H19. In the present study, we found that the protein level of SEMA6D was decreased after H19 interference, whereas H19 overexpression had the opposite effect. SEMA6D, a member of the semaphorin family, is an axon guiding factor (de Wit and Verhaagen, 2003) that can induce axon rejection. Semaphorins are signaling guidance molecules in the nervous system that regulate cell migration and cytoskeletal reorganization (Alto and Terman, 2017). At present, the two main receptors known to be involved in mediating semaphore responses are neuropilins and plexins (Raper, 2000),

which combine to transmit corresponding signals and activate downstream pathways. As the nervous system develops, the growth cone at the leading edge of the axon begins to extend toward its target. Axon guidance is controlled by different guidance signaling pathways, and semaphorin/plexin signaling induces a rejection response (Yang and Terman, 2013). SEMA6D is widely expressed in the brain from embryo to adult, and it may influence axon guidance and neuronal plasticity during development (Taniguchi and Shimizu, 2004). SEMA6D has been reported to induce the collapse of growth cones of DRG and hippocampal neurons (Qu et al., 2002). Studies have shown that SEMA6D works with its receptor plexinA1 (Toyofuku et al., 2004; Frank, 2006). Taking together our findings that H19 inhibited axon growth and SEMA6D protein expression was increased after H19 overexpression, and previous findings that SEMA6D can cause axon rejection, we suspect that H19 inhibits the growth of misdirected new axons by activating SEMA6D and inducing the collapse of growth cones after binding with receptors. Studies have shown that H19 acts as a competitive endogenous RNA to compete for binding to miRNA, acts as a molecular sponge, and plays a role in the proliferation and invasion of tumor cells (Lv et al., 2017; Qian et al., 2018). It can also bind to proteins to form complexes and mediate protein-protein interactions as a bridge (Luo et al., 2013; Ohtsuka et al., 2016). In this study, our findings indicate that it acts by activating downstream target genes.

In conclusion, our findings suggest that lncRNA H19 may regulate peripheral nerve degeneration and regeneration by activating SEMA6D in injured nerves. However, this study was based on a small sample size. The results did not investigate how lncRNA H19 plays a critical role in the treatment of neurological diseases. The findings of this study help to clarify the importance of lncRNA H19 in nerve regeneration and provide new ideas and a theoretical basis for further studies on the specific mechanism of H19 in nerve regeneration.

Author contributions: *YMF and JS performed experiments and interpreted the data. MC was responsible for gene expression analysis. YYZ conducted the animal studies. JS and MRJ performed data analysis. JS and YY performed immunohistochemical experiments. JXQ and ZHD analyzed functional and biochemical data. DBY analyzed the data, planned the study, supervised the project, and wrote the manuscript. All authors approved the final version of the manuscript.*

Conflicts of interest: *The authors declare that they have no competing interests.*

Availability of data and materials: *All data generated or analyzed during this study are included in this published article and its supplementary information files.*

Open peer reviewers: *Papon Muangsanit, National Science and Technology Development Agency, Thailand; Franck Sturtz, Limoges University, France.*

Additional files:

Additional Figure 1: *Flow chart of connecting silicone tubes.*

Additional Figure 2: *Flow chart of the experiment.*

Additional file 1: *Open peer review reports 1 and 2.*

References

Adriaenssens E, Dumont L, Lottin S, Bolle D, Leprêtre A, Delobelle A, Bouali F, Dugimont T, Coll J, Curgy JJ (1998) H19 overexpression in breast adenocarcinoma stromal cells is associated with tumor values and steroid receptor status but independent of p53 and Ki-67 expression. Am J Pathol 153:1597-1607.

Alto LT, Terman JR (2017) Semaphorins and their signaling mechanisms. Methods Mol Biol 1493:1-25.

Chan KM, Gordon T, Zochodne DW, Power HA (2014) Improving peripheral nerve regeneration: from molecular mechanisms to potential therapeutic targets. Exp Neurol 261:826-835.

Chen JS, Wang YF, Zhang XQ, Lv JM, Li Y, Liu XX, Xu TP (2016) H19 serves as a diagnostic biomarker and up-regulation of H19 expression contributes to poor prognosis in patients with gastric cancer. Neoplasma 63:223-230.

Chen P, Piao X, Bonaldo P (2015) Role of macrophages in Wallerian degeneration and axonal regeneration after peripheral nerve injury. Acta Neuropathol 130:605-618.

de Wit J, Verhaagen J (2003) Role of semaphorins in the adult nervous system. Prog Neurobiol 71:249-267.

Dharap A, Bowen K, Place R, Li LC, Vemuganti R (2009) Transient focal ischemia induces extensive temporal changes in rat cerebral microRNAome. J Cereb Blood Flow Metab 29:675-687.

Duan RS, Liu PP, Xi F, Wang WH, Tang GB, Wang RY, Saijilafu, Liu CM (2018) Wnt3 and Gata4 regulate axon regeneration in adult mouse DRG neurons. Biochem Biophys Res Commun 499:246-252.

Dubový P (2011) Wallerian degeneration and peripheral nerve conditions for both axonal regeneration and neuropathic pain induction. Ann Anat 193:267-275.

Esteller M (2011) Non-coding RNAs in human disease. Nat Rev Genet 12:861-874.

Fatica A, Bozzoni I (2014) Long non-coding RNAs: new players in cell differentiation and development. Nat Rev Genet 15:7-21.

Feigenberg T, Gofrit ON, Pizov G, Hochberg A, Benshushan A (2013) Expression of the h19 oncofetal gene in premalignant lesions of cervical cancer: a potential targeting approach for development of nonsurgical treatment of high-risk lesions. ISRN Obstet Gynecol 2013:137509.

Feil R, Walter J, Allen ND, Reik W (1994) Developmental control of allelic methylation in the imprinted mouse Igf2 and H19 genes. Development 120:2933-2943.

Frank E (2006) Axon guidance in the spinal cord: choosin' by exclusion. Neuron 52:745-746.

Geuna S, Raimondo S, Ronchi G, Di Scipio F, Tos P, Czaja K, Fornaro M (2009) Chapter 3: Histology of the peripheral nerve and changes occurring during nerve regeneration. Int Rev Neurobiol 87:27-46.

Gibb EA, Brown CJ, Lam WL (2011) The functional role of long non-coding RNA in human carcinomas. Mol Cancer 10:38.

Gordon T (2020) Peripheral Nerve Regeneration and Muscle Reinnervation. Int J Mol Sci 21:8652.

Gu Y, Wu Y, Su W, Xing L, Shen Y, He X, Li L, Yuan Y, Tang X, Chen G (2018) 17β-estradiol enhances Schwann cell differentiation via the ERβ-ERK1/2 signaling pathway and promotes remyelination in injured sciatic nerves. Front Pharmacol 9:1026.

Huang Z, Lei W, Hu HB, Zhang H, Zhu Y (2018) H19 promotes non-small-cell lung cancer (NSCLC) development through STAT3 signaling via sponging miR-17. J Cell Physiol 233:6768-6776.

Li L, Xu Y, Wang X, Liu J, Hu X, Tan D, Li Z, Guo J (2021) Ascorbic acid accelerates Wallerian degeneration after peripheral nerve injury. Neural Regen Res 16:1078-1085.

Li S, Hua Y, Jin J, Wang H, Du M, Zhu L, Chu H, Zhang Z, Wang M (2016) Association of genetic variants in lncRNA H19 with risk of colorectal cancer in a Chinese population. Oncotarget 7:25470-25477.

Li Y, Sun Y, Cai M, Zhang H, Gao N, Huang H, Cui S, Yao D (2018) Fas ligand gene (Faslg) plays an important role in nerve degeneration and regeneration after rat sciatic nerve injury. Front Mol Neurosci 11:210.

Li Y, Cai M, Feng Y, Yung B, Wang Y, Gao N, Xu X, Zhang H, Huang H, Yao D (2022) Effect of lncRNA H19 on nerve degeneration and regeneration after sciatic nerve injury in rats. Dev Neurobiol 82:98-111.

Lu Y, Shan Q, Ling M, Ni XA, Mao SS, Yu B, Cao QQ (2022) Identification of key genes involved in axon regeneration and Wallerian degeneration by weighted gene co-expression network analysis. Neural Regen Res 17:911-919.

Luo M, Li Z, Wang W, Zeng Y, Liu Z, Qiu J (2013) Long non-coding RNA H19 increases bladder cancer metastasis by associating with EZH2 and inhibiting E-cadherin expression. Cancer Lett 333:213-221.

Lv M, Zhong Z, Huang M, Tian Q, Jiang R, Chen J (2017) lncRNA H19 regulates epithelial-mesenchymal transition and metastasis of bladder cancer by miR-29b-3p as competing endogenous RNA. Biochim Biophys Acta Mol Cell Res 1864:1887-1899.

Matouk IJ, Halle D, Gilon M, Hochberg A (2015) The non-coding RNAs of the H19-IGF2 imprinted loci: a focus on biological roles and therapeutic potential in Lung Cancer. J Transl Med 13:113.

National Research Council of the National Academies (2011) Guide for the care and use of laboratory animals (8th ed).

Navarro X, Vivó M, Valero-Cabré A (2007) Neural plasticity after peripheral nerve injury and regeneration. Prog Neurobiol 82:163-201.

Niu ZS, Niu XJ, Wang WH (2017) Long non-coding RNAs in hepatocellular carcinoma: Potential roles and clinical implications. World J Gastroenterol 23:5860-5874.

Nocera G, Jacob C (2020) Mechanisms of Schwann cell plasticity involved in peripheral nerve repair after injury. Cell Mol Life Sci 77:3977-3989.

Ohtsuka M, Ling H, Ivan C, Pichler M, Matsushita D, Goblirsch M, Stiegelbauer V, Shigeyasu K, Zhang X, Chen M, Vidhu F, Bartholomeusz GA, Toiyama Y, Kusunoki M, Doki Y, Mori M, Song S, Gunther JR, Krishnan S, Slaby O, et al. (2016) H19 noncoding RNA, an independent prognostic factor, regulates essential Rb-E2F and CDK8-β-catenin signaling in colorectal cancer. EBioMedicine 13:113-124.

Peng L, Yuan XQ, Liu ZY, Li WL, Zhang CY, Zhang YQ, Pan X, Chen J, Li YH, Li GC (2017) High lncRNA H19 expression as prognostic indicator: data mining in female cancers and polling analysis in non-female cancers. Oncotarget 8:1655-1667.

Peng Z, Liu C, Wu M (2018) New insights into long noncoding RNAs and their roles in glioma. Mol Cancer 17:61.

Percie du Sert N, Hurst V, Ahluwalia A, Alam S, Avey MT, Baker M, Browne WJ, Clark A, Cuthill IC, Dirnagl U, Emerson M, Garner P, Holgate ST, Howells DW, Karp NA, Lazic SE, Lidster K, MacCallum CJ, Macleod M, Pearl EJ, et al. (2020) The ARRIVE guidelines 2.0: Updated guidelines for reporting animal research. PLoS Biol 18:e3000410.

Qian B, Wang DM, Gu XS, Zhou K, Wu J, Zhang CY, He XY (2018) LncRNA H19 serves as a ceRNA and participates in non-small cell lung cancer development by regulating microRNA-107. Eur Rev Med Pharmacol Sci 22:5946-5953.

Qu X, Wei H, Zhai Y, Que H, Chen Q, Tang F, Wu Y, Xing G, Zhu Y, Liu S, Fan M, He F (2002) Identification, characterization, and functional study of the two novel human members of the semaphorin gene family. J Biol Chem 277:35574-35585.

Raper JA (2000) Semaphorins and their receptors in vertebrates and invertebrates. Curr Opin Neurobiol 10:88-94.

Rinn JL, Chang HY (2012) Genome regulation by long noncoding RNAs. Annu Rev Biochem 81:145-166.

Robinson LR (2000) Traumatic injury to peripheral nerves. Muscle Nerve 23:863-873.

Shi Z, Ning G, Zhang B, Yuan S, Zhou H, Pan B, Li J, Wei Z, Cao F, Kong X, Feng S (2019) Signatures of altered long noncoding RNAs and messenger RNAs expression in the early acute phase of spinal cord injury. J Cell Physiol 234:8918-8927.

Siemionow M, Brzezicki G (2009) Chapter 8: Current techniques and concepts in peripheral nerve repair. Int Rev Neurobiol 87:141-172.

Spinelli M, Boucard C, Ornaghi S, Schoeberlein A, Irene K, Coman D, Hyder F, Zhang L, Haesler V, Bordey A, Barnea E, Paidas M, Surbek D, Mueller M (2021) Preimplantation factor modulates oligodendrocytes by H19-induced demethylation of NCOR2. JCI Insight 6:e132335.

Tang BL (2020) Axon regeneration induced by environmental enrichment- epigenetic mechanisms. Neural Regen Res 15:10-15.

Tang H, Brimijoin S (2002) Death of preganglionic sympathetic neurons after surgical or immunologic lesion of peripheral processes. Exp Neurol 177:105-114.

Tang S, Zhu J, Xu Y, Xiang AP, Jiang MH, Quan D (2013) The effects of gradients of nerve growth factor immobilized PCLA scaffolds on neurite outgrowth in vitro and peripheral nerve regeneration in rats. Biomaterials 34:7086-7096.

Taniguchi M, Shimizu T (2004) Characterization of a novel member of murine semaphorin family. Biochem Biophys Res Commun 314:242-248.

Toyofuku T, Zhang H, Kumanogoh A, Takegahara N, Suto F, Kamei J, Aoki K, Yabuki M, Hori M, Fujisawa H, Kikutani H (2004) Dual roles of Sema6D in cardiac morphogenesis through region-specific association of its receptor, Plexin-A1, with off-track and vascular endothelial growth factor receptor type 2. Genes Dev 18:435-447.

Wan P, Su W, Zhuo Y (2017) The Role of Long Noncoding RNAs in Neurodegenerative Diseases. Mol Neurobiol 54:2012-2021.

Wang L, Cai Y, Zhao X, Jia X, Zhang J, Liu J, Zhen H, Wang T, Tang X, Liu Y, Wang J (2015) Down-regulated long non-coding RNA H19 inhibits carcinogenesis of renal cell carcinoma. Neoplasma 62:412-418.

Wu P, Zuo X, Deng H, Liu X, Liu L, Ji A (2013) Roles of long noncoding RNAs in brain development, functional diversification and neurodegenerative diseases. Brain Res Bull 97:69-80.

Yang T, Terman JR (2013) Regulating small G protein signaling to coordinate axon adhesion and repulsion. Small GTPases 4:34-41.

Zhao L, Li Z, Chen W, Zhai W, Pan J, Pang H, Li X (2017) H19 promotes endometrial cancer progression by modulating epithelial-mesenchymal transition. Oncol Lett 13:363-369.

Zhou Y, Zhang Y (2020) Inhibition of LncRNAH19 has the effect of anti-tumour and enhancing sensitivity to gefitinib and chemotherapy in non-small-cell lung cancer in vivo. J Cell Mol Med 24:5811-5816.

P-Reviewers: Muangsanit P, Sturtz F; C-Editor: Zhao M; S-Editors: Yu J, Li CH; L-Editors: McCollum L, Song LP; T-Editor: Jia Y

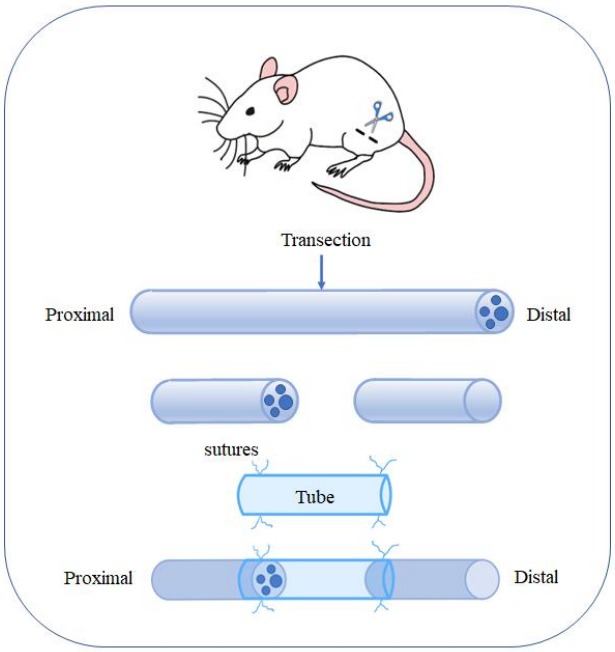

Additional Figure 1 Flow chart of connecting silicone tube.

Sciatic nerve was transected 14 days after injection of Adeno-associated virus, and both ends of sciatic nerve stump were connected with silicone tube. Sciatic nerve wrapped by silicone tube was removed 14 days later, and the growth of axons was observed by sectionalized staining.

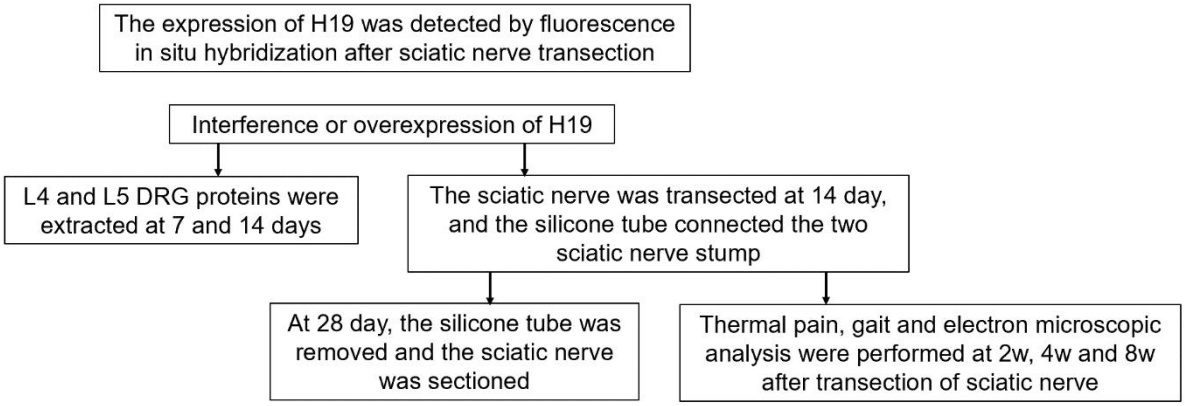

Additional Figure 2 Flow chart of the experiment.

DRG: Dorsal root ganglion; H19: long noncoding RNA H19.